J. Phys.: Condens. Matter **11** (1999) 6079–6098. Printed in the UK PII: S0953-8984(99)02735-6

Can the isotopic H↔D substitution affect the conformational properties of polymeric aqueous solutions? The poly(ethylene oxide)–water case

C Branca†, A Faraone†, G Maisano†, S Magazù†, P Migliardo†, A Triolo‡, R Triolo‡ and V Villari†

† Dipartimento di Fisica and INFM, Università di Messina, PO Box 55, Papardo, 98166 S. Agata di Messina, Italy

‡ Dipartimento di Chimica-Fisica and INFM, Università di Palermo, V. le delle Science, Parco d'Orleans II, 90128, Palermo, Italy

Received 17 March 1999, in final form 17 May 1999

Abstract. This paper deals with measurements, performed using dynamic light scattering (photon correlation spectroscopy (PCS) and Raman spectroscopy) and small angle neutron scattering (SANS), on solutions of poly(ethylene oxide) (PEO) in water and heavy water. The joint employment of these techniques allows us to carry out a side by side comparison between the PEO/H_2O and the PEO/D_2O systems. The coil conformation dependence on temperature and concentration is studied; in particular, the hydrodynamic radius, as evaluated from the diffusion coefficient at infinite dilution using PCS, and the gyration radius, evaluated by SANS, are determined at different temperatures, i.e. as a function of the solvent quality. On the other, the study of the Raman D-LAM spectral contribution furnishes valuable information on the structural arrangement of the molecules.

The experimental findings clearly show from the different diffusive properties of polymer chains that the isotopic substitution affects the hydrodynamic radius behaviour with temperature, and from the Raman scattering results that it induces a lowering of the conformational order degree. Such findings provide evidence of the different behavioural properties of macromolecules in H_2O and D_2O, and could be relevant for the areas of research in which the deuterium labelling technique is commonly employed.

1. Introduction

In recent years much attention has been paid to poly(ethylene oxide) (PEO) [1, 2]. This synthetic polymer is of relevant importance in polymer physics, both for the simplicity of its fundamental repeating unit –(CH_2–CH_2–O)–, which makes it a good model for the study of more complex polymeric systems, and for those features (e.g. its drag reducing properties) for which it is employed in a wide variety of applications. Moreover PEO shows some peculiar properties of great interest; for example, unlike other polyepoxides (general formula $[(CH_2)_xO]_n$, for PEO $x = 2$), it is soluble both in common organic solvents, like the other members of the series, and in water. This characteristic behaviour seems to be ought to a crucial balance of the hydrophobic forces exerted by the ethylene units, –CH_2–CH_2–, with the hydrophilic interaction of the oxygens contained in the oxirane units and in the terminal groups. These latter play an important role in the shortest chains, their importance decreasing when the polymerization degree n increases. The resultant of these two competitive forces, hydrophilic and hydrophobic, makes PEO soluble in water in all proportions at temperature

0953-8984/99/326079+20$30.00

lower than the boiling point of water; above this point it presents a miscibility gap that, by diminishing n, shifts towards higher temperatures and vanishes for $n < 48$.

As far as PEO molecule conformation is concerned, it is well stated that in the crystalline state PEO assumes a helical conformation (like other important biological systems, e.g. DNA) that contains seven structural units CH_2–CH_2–O with two helical turns per fibre identity period (19.3 Å), i.e. 7_2 helix structure [3, 4]. Previous works have reported experimental evidences which support the hypothesis that PEO retains some of its helicity even in dilute aqueous solutions [5, 6], assuming in the presence of water a more ordered conformation with respect to the one in the melt state. Moreover the similarity of the ether oxygen spacing (2.88 Å) to that of the oxygens in water (2.85 Å) evidently provides a good structural fit of the PEO coil to the water H-bonding network. These two occurrences could be related to the unusual ability, assessed by Devanand and Selser [7], of water molecules to 'pack' into and swell coils along with a general structuring of water in the PEO/H_2O system. As a result the second osmotic virial coefficient A_2 and the prefactor a in the scaling relation $R_g = an^{\nu}$ are unusually large for PEO in water, indicating that water is an extremely good solvent for PEO. However in a recent work of Bieze *et al* [8] the hypothesis that PEO can be hydrated by an unperturbed tetrahedral water lattice is refused and no evidence of structured water at the polymer interface is observed.

The aim of the present work is to study the conformational properties of PEO chain in the two solvents H_2O and D_2O. In this frame, it is well known that deuterium labelling plays an essential role in many areas of research where a purely massive effect is attributed to the H/D substitution. In contrast with this assumption many experimental anomalies have been observed near phase boundaries and in particular near critical points, where the overall interactions are delicately balanced and, therefore, even small additional contributions can shift the critical temperature significantly [9, 10]. We will show that, also far from these conditions, in PEO aqueous solutions, the H_2O/D_2O solvent substitution affects significantly the conformational behaviour of the polymer and its temperature dependence.

2. Theoretical background

The phase diagram of PEO aqueous solutions has been studied with particular interest by several authors because some peculiar properties, as for example the presence of a low critical solution temperature (LCST), cannot be explained by the simple Flory theory [11–13]. In this section some of the theoretical models able to describe the PEO phase diagram will be briefly reviewed.

The early theory of Kjellander and Florin (KF) to elucidate the phase behaviour of PEO aqueous solutions [14] is based on the hypothesis of a good structural fit between water and polymer molecules. PEO molecules are thought to be engaged in a hexagonal water structure (ice I_h structure): all the ether oxygens of the polymer chain replace some of the oxygens in the water structure and are bound to the lattice with hydrogen bonds. This picture is sustained by the occurrence that, as already mentioned, the distance between the oxygen atoms in the PEO helical conformation and in the water hydrogen-bonded tetrahedral coordination is nearly the same. Indeed the hypothesis of an enhanced water structure around the chain could explain the experimental findings that both the entropy and the enthalpy of mixing are negative in PEO/H_2O solutions; the structuring of water around PEO should be entropically unfavourable but this latter contribution in the free energy is overcome by the enthalpic one. The good structural fit is fundamental in making the enthalpy contribution sufficiently large and would explain why the other polyethers are not soluble in water. In the KF theory [14] a parameter, w, is introduced to take into account polymer–polymer contacts and hydration shell overlaps.

It plays, essentially, the role of the χ parameter of the Flory theory in describing the solvent quality. KF calculations indicate that w decreases monotonically as temperature is raised making the solvent poorer. This behaviour can be rationalized by hypothesizing that the energetically stabilized hydration shells around the polymer chains break down as temperature is increased. The phase separation at the LCST is considered to be due to the rupture of the balance between the entropic and enthalpic contributions; the former becomes increasingly more important at higher temperature even if its absolute value decreases because of the hydration shell breaking down; the latter decreases in absolute value too; if the structure does not break down sufficiently rapidly when the temperature is raised, the unfavourable entropy contribution soon dominates and the system phase separates.

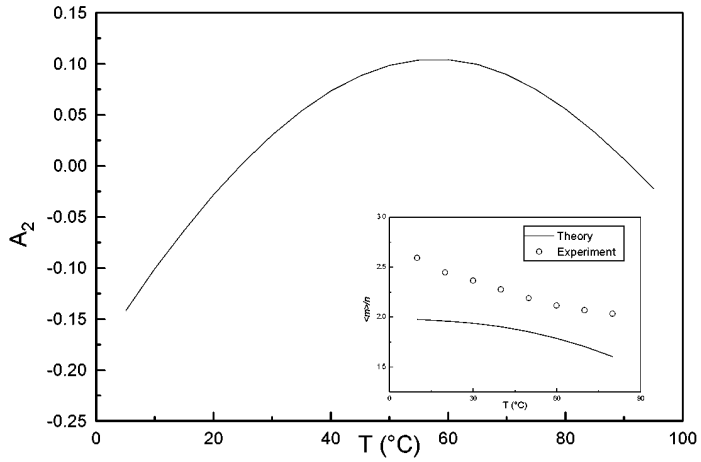

Figure 1. Matsuyama and Tanaka theory results for A_2. In the inset the temperature behaviour of the average hydration number/polymerization degree ratio, as obtained by MT theory and ultrasonic velocity measurements, is reported.

A different picture, in which the phase diagram for the PEO/water system has been calculated using Flory–Huggins theory assuming that each segment of the PEO chain may exist in two forms due to the rotations around C–C and C–O bonds, was proposed by Karlström [15]. There exists theoretical and experimental support for the idea that the oxygens prefer a *gauche* orientation around the C–C bond and that a *trans* conformation is preferred around the C–O bonds. Such an orientation creates a segment of the PEO chain which has a rather large dipole moment and could be expected to interact favourably with water, whereas other conformations will have smaller or no dipole moments and can be assumed to interact less favourably with water. Changing temperature the probability distribution corresponding to the *gauche* and *trans* conformation varies and modifies the PEO–water interaction. Using this model a semiquantitative agreement with the experiment is achieved.

More recently Matsuyama and Tanaka developed a theory [16] (MT) to describe LCST in polymer solutions and applied it to PEO aqueous solutions. The model is based on the assumption that each monomer is able to form P physical bonds with the solvent. Since the interaction energy is of the order of thermal energy, the bonding–unbonding equilibrium is easily established by thermal activation. The system is defined as formed by m clusters (i.e. m solvent molecules attached to a polymer molecule), each cluster being considered as a separate chemical species, and by free solvent molecules. Applying the Flory–Huggins theory to the system formed by the m clusters and by the solvent, the distribution of m can be determined.

The resulting average number $\langle m \rangle$ of the solvent molecules bonded to the polymer decreases with temperature, causing a worsening in the solvent quality and, at a certain temperature, to a phase separation. Matsuyama and Tanaka used this model to fit, with a good accuracy, the phase diagram of PEO/H_2O solutions assuming $P = 1$ and introducing four free parameters [16]. Figure 1 shows the second virial coefficient, as obtained by MT. In the inset the $\langle m \rangle / n$ behaviour as a function of temperature, obtained using a value of $P = 2$, is compared with the data obtained by previous ultrasonic velocity measurements [17]. The choice $P = 2$, instead of $P = 1$ as in the Matsuyama and Tanaka paper, has been made solely to allow a more direct comparison with the experimental results on the hydration number. It should be stressed that different experimental techniques can furnish different values of the number of water molecules which are thought to be present at the PEO hydration shell.

As far as the theoretical behaviour of A_2 is concerned, it presents a maximum at about 60 °C; this result is in contrast with previous experimental findings [1]. However, changing the value of the parameters involved in the calculation, for example P, the maximum shifts towards lower or higher temperatures. Recently the MT theory has been successfully employed in the study of PEO aqueous solutions [18]; however it does not explain why other polyethers are not soluble in water and does not take into account the evidence that PEO in water partially retains the 7_2 helix structure.

3. Experimental set-up

The solutions were freshly prepared from standard PEO samples with average molecular weight $M_w = 3400$ Da, using ultrapure H_2O and D_2O. PEO solutions were filtered in recirculation through 0.22 μm (nominal pore size) Millipore PTFE filter. Great care was taken in order to obtain stable, clear and dust free samples. The samples were sealed in optical quartz cells, and then mounted in an optical thermostat stabilizing temperatures within ± 0.1 °C.

3.1. PCS measurements

PCS measurements were performed using a photon counting optical system and a Brookhaven BI-2030 correlator to analyse the scattered light. As exciting source, the 4880 Å vertically polarized line of an Innova unimode Ar^+ laser model 70, working in the power range of 50–400 mW, was used. The scattered light, by means of an optical fibre, was detected in a 90° scattering geometry. The intensity–intensity autocorrelation functions were analysed with a standard cumulant analysis. All the measurements were performed in the $kR_g \ll 1$ region where no internal modes contribute to the correlation function.

It is well known that the experimentally measured quantity in a PCS experiment, working in a homodyne geometry, is the scattered intensity autocorrelation function $\langle I(0)I(t) \rangle$. Under the hypothesis of samples consisting of a large number of independent scatterers, the Siegert relation [19] can be applied:

$$g^{(2)}(t) = 1 + b|g^{(1)}(t)|^2 \tag{1}$$

where b is an optical parameter. Equation (1) links the second order correlation function $g^{(2)}(t) = \langle I(0)I(t) \rangle / \langle I \rangle^2$, namely the intensity autocorrelation function normalized to the square of the average intensity, i.e. to the first order correlation function $g^{(1)}(t)$, defined as $g^{(1)}(t) = \langle E_S(0)E_S(t) \rangle / \langle I \rangle$. If the scatterers are monodisperse, isotropic and in a dilute solution, it can be demonstrated that:

$$g^{(1)}(t) = \exp(-Dk^2 t) \tag{2}$$

$k = (4\pi n/\lambda) \sin(\theta/2)$ being the scattered wave vector and D being the diffusion coefficient.

At low concentration, for the k values and the scatterers' mutual distance involved in the present experiment, $D(k)$ represents the collective diffusion, $D(k \to 0) = D_c$, determined both by hydrodynamic and structural contributions [20]:

$$D(k \to 0) = D_c = D_0 \frac{H(0)}{S(0)} \tag{3}$$

where $S(k)$ and $H(k)$ are the structure factor and the hydrodynamic function respectively and $S(0) = S(k \to 0)$ and $H(0) = H(k \to 0)$ are their values in the limit of $k \to 0$.

Extrapolating the data to zero concentration, the infinite dilution diffusion coefficient D_0, i.e. the diffusion coefficient of the isolated particle, can be obtained. The hydrodynamic radius can be calculated from D_0 using the Einstein–Stokes (ES) relation:

$$R_H = \frac{k_B T}{6\pi\eta D_0} \tag{4}$$

where η is the solvent viscosity and R_H represents the radius of the entity constituted by the scatterer and its hydration shell.

If some polydispersity is present a standard cumulant analysis [19] is more suitable for the fitting of $g^{(1)}(t)$:

$$\ln g^{(1)}(t) = -D_{eff} k^2 t + \tfrac{1}{2}\mu_2 t^2 + \cdots. \tag{5}$$

In equation (5), D_{eff} is the collective diffusion coefficient, averaged over the distribution of particle size weighted by the square mass.

The measure of the effective diffusion coefficient at different concentration values furnishes fundamental information about the investigated system. In fact, the concentration dependence of D_c can be examined through the Gibbs–Duhem expression [21]:

$$D_c = \frac{k_B T}{\zeta_{ch}} \left(1 - \frac{N_A V_1}{M} c\right) (1 + 2A_2 M c) \tag{6}$$

where ζ_{ch} is the frictional coefficient of the polymer molecule in solution, which, in the limit of infinite dilution, takes the Einstein–Stokes form $\zeta_0 = 6\pi\eta R_H$. The second term in parenthesis is the virial expansion of the structure factor, A_2 is the second virial coefficient of the osmotic pressure, M is the molecular mass, N_A is the Avogadro number and V_1 is the partial specific volume of the polymer. In equation (6) the concentration dependence of D_c is separated into two parts: the first contribution originates from the chemical potential, involved in the virial coefficient; the second contribution is due to the hydrodynamic interaction, which is included in the frictional coefficient ζ_{ch}. From equation (6) it can be further concluded that the concentration dependence of D_c can be nonzero at the θ condition because, even if A_2 vanishes, ζ_{ch} may be still concentration dependent. In the theoretical calculations, the concentration dependence of D_c is normally expressed as [21]:

$$D_c(c) = D_0(1 + k_D c) \tag{7}$$

where k_D depends on the relative magnitudes of A_2 and of the first order concentration coefficient of the virial expansion of ζ_{ch}. For this reason the relation linking k_D to A_2 is usually written [22]:

$$k_D = 2A_2 M - k_f - V_1 \tag{8}$$

where k_f is the friction coefficient and V_1 is usually small and can be neglected.

3.2. Raman measurements

Polarized (I_{VV}) and depolarized (I_{VH}) Raman spectra were obtained by a Spex Ramalog 5 triple monochromator in a 90° scattering geometry in the −40–80 °C temperature range, using the 5145 Å line of an Ar^+ laser. The laser power was maintained at approximately 5 W. The scattered photons were automatically normalized for the incoming beam intensity in order to ensure good data reproducibility. The samples were sealed in optical quartz cells and then mounted in an optical thermostat which stabilizes temperature within ±0.1 °C. The spectral range covered was 200–400 cm^{-1} with an instrumental resolution of 2 cm^{-1}. The investigated values of temperature and concentration both in H_2O and D_2O are reported in table 1.

Table 1. Concentration values, c (g cm^{-3}), corresponding to the ratio n_w/n_p between the number of water and polymer molecules respectively, for the temperatures and concentrations investigated in Raman measurements.

	c (g cm^{-3})			
n_w/n_p	$T = 20$ °C	$T = 30$ °C	$T = 45$ °C	$T = 60$ °C
20	1.03	1.01	1.00	0.99
100	0.73	0.72	0.71	0.70
200	0.53	0.53	0.52	0.51
280	0.43	0.43	0.43	0.42
350	0.37	0.37	0.37	0.36

The spectral information which matters most in this study are the isotropic scattering intensities, calculated from the parallel and perpendicular components of the scattered light. By polarization analysis, the different polarization character of the spectral contributions can be put in evidence through the evaluation of the isotropic contribution:

$$I_{ISO} = I_{VV} - 4/3 I_{VH}. \tag{9}$$

As far as the strongly polarized longitudinal acoustic mode (LAM) of polymers is concerned, it is commonly attributed to many contributions representing the polymer skeletal bending and stretching vibrations [23]. In the elastic rod model, which can be used for crystalline systems, the LAM centre frequencies are related to the stem length l_K by the formula [24]:

$$\omega_{LAM} = k\nu = \frac{1}{l_K}\sqrt{\frac{E}{\rho}} \tag{10}$$

where E and ρ are the elastic modulus and density respectively, and where $\nu = \sqrt{E/\rho}$ is the propagating velocity of the longitudinal perturbation.

In non-crystalline systems the narrow LAM band is replaced by the much broader polarized band associated to the disordered longitudinal acoustic mode (D-LAM) [25]. In such a case, in equation (10), l_K is the Kuhn statistical segment length which is a measure of the polymer flexibility, and can be expressed in terms of the ratio between the square of the polymer coil radius, R, and its maximum possible value, R_{max} : $l_k = R^2/R_{max}$. The broadening of the D-LAM band must be attributed to the conformational disorder of the non-crystalline systems.

The D-LAM bands have been fitted by the log-normal functional form:

$$I(\omega) = A \exp\left[-\frac{1}{2}\left(\frac{\ln(\omega/\omega_{D\text{-}LAM})}{\gamma_{D\text{-}LAM}}\right)^2\right] \tag{11}$$

where A is the amplitude, $\omega_{D\text{-}LAM}$ the band centre frequency and $\gamma_{D\text{-}LAM}$ the width of the distribution. The log-normal function has been chosen because it is the function that better fit the strongly non-symmetrical profile of the bands. The asymmetry [26, 27] of the bands arises from the fact that the D-LAM contribution results from a non-homogeneous overlapping of sub-bands due to the many different conformers in the sample.

3.3. SANS measurements

SANS data on D_2O solutions of PEO 3400 were collected on the 30 m instrument of the WC Koehler Scattering Centre of Oak Ridge National Laboratory (USA). Samples were held in quartz spectrophotometric cells (pathlength 2 mm). A sample–detector distance of 1.52 m, combined with the 4 cm beam stop, and neutrons of mean wavelength of 4.75 Å ($\Delta\lambda/\lambda \sim 5\%$) gave a range of momentum transfer 0.03–0.38 $Å^{-1}$. In all cases the two dimensional scattering contours, corrected for detector efficiency, instrumental background etc, were isotropic and therefore were reduced to 1D radial averages which were converted to scattering cross sections per unit volume (cm^{-1}) using water as secondary calibration standard. Temperature was controlled within 0.2 °C by means of an external bath.

It is well known that, in a SANS experiment, the coherent differential scattering cross section of a solution of monodisperse and centrosymmetric particles, under the hypothesis of independence of intermolecular and intramolecular averages, can be separated into three terms [28]:

$$\left(\frac{\mathrm{d}\sigma(k)}{\mathrm{d}\Omega}\right)_{coh} = nP(k)S(k) \tag{12}$$

where n is the number density, and $P(k)$ and $S(k)$ are the form and structure factor respectively. Under the assumption that the distribution of the monomer in the coil is Gaussian the form factor of an ideal polymer chain can be simply derived:

$$P(k) = \left|\int_V (\rho - \rho_0)\exp(\mathrm{i}k\cdot r)\,\mathrm{d}V\right|^2 = K^2V^2 f(kR_g)$$
$$= K^2V^2\frac{2}{(kR_g)^4}(\exp(-(kR_g)^2) - 1 + (kR_g)^2) \tag{13}$$

where the integral is on the volume of the particle V, ρ and ρ_0 are the coherent scattering length densities of the particle and solvent respectively, $K = \rho - \rho_0$, $f(x)$ is the Debye form factor [29] for a random coil and R_g is the gyration radius. In a dilute solution interparticle interactions can be neglected and the structure factor can be approximated to 1; as a consequence the spectra result simply proportional, through the number concentration, to the form factor.

From equation (12) the Zimm plot method for the analysis of static intensity measurements can be simply derived. In the limit of low k values and dilute solution, the form factor can be approximated by the expression $P(k) = K^2V^2(1 + R_g^2k^2/3)$ and the structure factor can be approximated to its value at $k = 0$, $S(0)$. $S(0)$ is the inverse of the osmotic pressure and can be expressed using a virial expansion. This results in

$$\frac{c}{(\mathrm{d}\sigma(k)/\mathrm{d}\Omega)_{coh}} = \frac{M}{K^2V^2}\left(1 + \frac{k^2R_g^2}{3}\right)(1 + 2A_2Mc). \tag{14}$$

The experimental data of intensity have been fitted using the Debye form factor. However, increasing concentration, interactions between the polymer chains must be taken into account. To determine the value of A_2 equation (14) has been used. The value of c/I in the limit of $k \to 0$ has been calculated according to the Guinier approximation (equation (14)) and the resulting c/I versus c data have been fitted using a linear regression.

4. Results and discussion

PCS measurements have been performed on PEO 3400 at different concentration and temperature values. The chosen concentrations are all in the dilute region according to the condition reported in the literature [21]:

$$c < c^* \cong \frac{3M}{4\pi N_A R_g^3} \tag{15}$$

where c^* is the overlapping concentration. In equation (15) the R_g values were obtained from the SANS data.

As far as the PEO 3400/H_2O solutions are concerned, figure 2 shows the effective diffusion coefficient data as a function of concentration at some of the investigated temperatures. The straight lines in figure 2 are the best fit according to equation (7). It is well stated, according to previous findings in polymeric and colloidal systems, and to computer simulation experiments [30–32], that a positive slope of the initial dependence of the diffusion coefficient on concentration indicates the existence of repulsive interactions among the particles; a fairly independent behaviour with concentration signals a nearly theta condition and, finally, a negative slope indicates that attractive interactions are present in the system. This interpretation of the data is in agreement with the theoretical landscape sketched in the previous sections according to the Gibbs–Duhem expression (equation (6)).

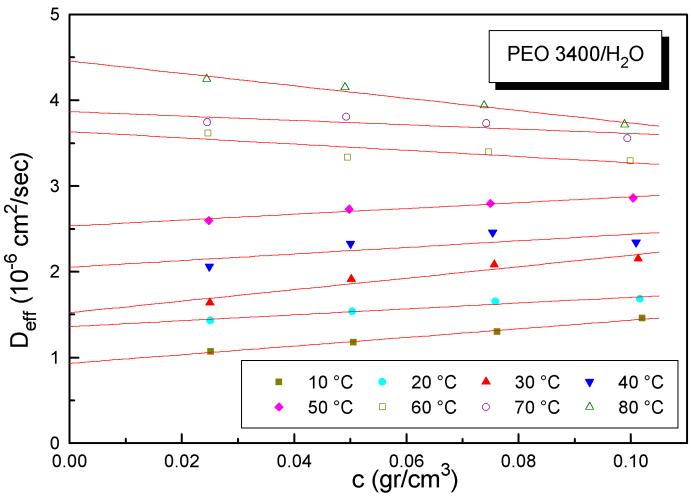

Figure 2. Concentration dependence of the effective diffusion coefficient for PEO 3400/H_2O solutions at various temperatures.

From the extrapolated values of D_0, the hydrodynamic radius has been determined for different temperature values. The obtained results are reported in figure 3(a). It is evident that different regimes can be distinguished. In the first one, from 5 to 15–20 °C, R_H increases with temperature; then it saturates in the range between 20 and 40 °C and, finally, from 40 to 80 °C, it slightly decreases with increasing temperature. This result can be better interpreted considering also the temperature behaviour of k_D, which is reported in figure 4(a). The trend of k_D is similar to that of R_H: it increases with temperature until 20 °C and decreases from 25 to 80 °C. Both the results can be interpreted in terms of a temperature dependent solvent quality of water. To rationalize these results one should bear in mind that the amount of water

for each polymer molecule decreases with increasing temperature, as shown by Mandelstam–Brillouin light scattering and by ultrasonic measurements [17] (see inset of figure 1). This can be ascribed to the enhanced thermal motions at higher temperature that lead to lower residence times of water molecules in the nearby hydration of the polymer. As a consequence, the average number of water molecules moving together with the polymer will be lower. At the same time, it should be also pointed out that with increasing temperature, owing to the rupture of a certain fraction of hydrogen bonds in water, the number of water molecules available for bonding with the polymer increases too. Finally, as already mentioned in the previous section, the excluded volume interactions, for increasing values of temperature, increase and tend to swell the polymer structure. Therefore, the hydrodynamic radius behaviour as a function of temperature is determined by the net result of these three effects. Our results indicate, at low temperatures, a major incidence of the intramolecular repulsive interaction between the constituent monomeric units, then an equilibrium, and, at high temperatures, an effect of apparent shrinking of the PEO coil also due to the loss of water molecules. This interpretation is in agreement with MT theory.

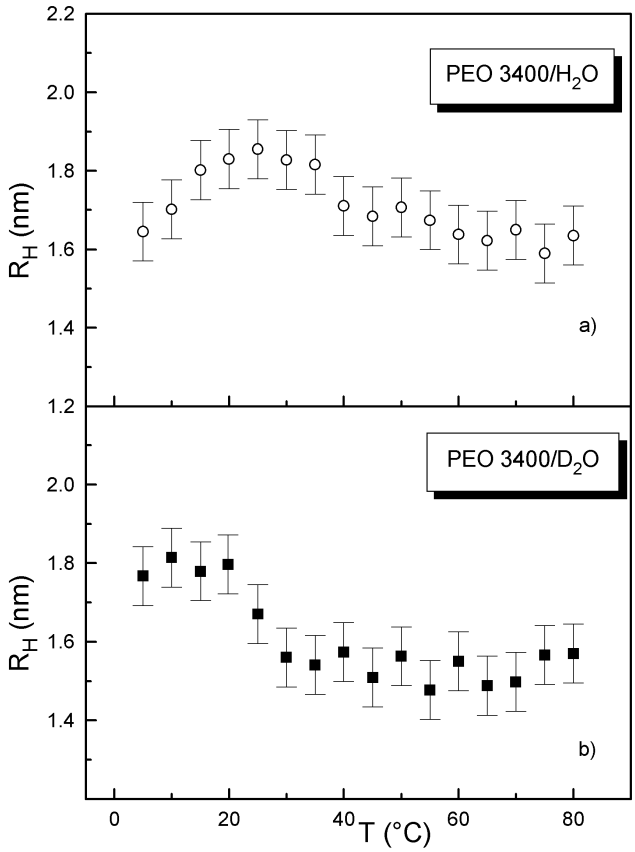

Figure 3. (a) Temperature dependence of the hydrodynamic radius for PEO 3400/H_2O solutions. (b) Temperature dependence of the hydrodynamic radius for PEO 3400/D_2O solutions.

As far as the k_D behaviour is concerned, it can be explained by a temperature dependent solvent power of H_2O. This finding is in accordance with the behaviour of Mark–Houwink–

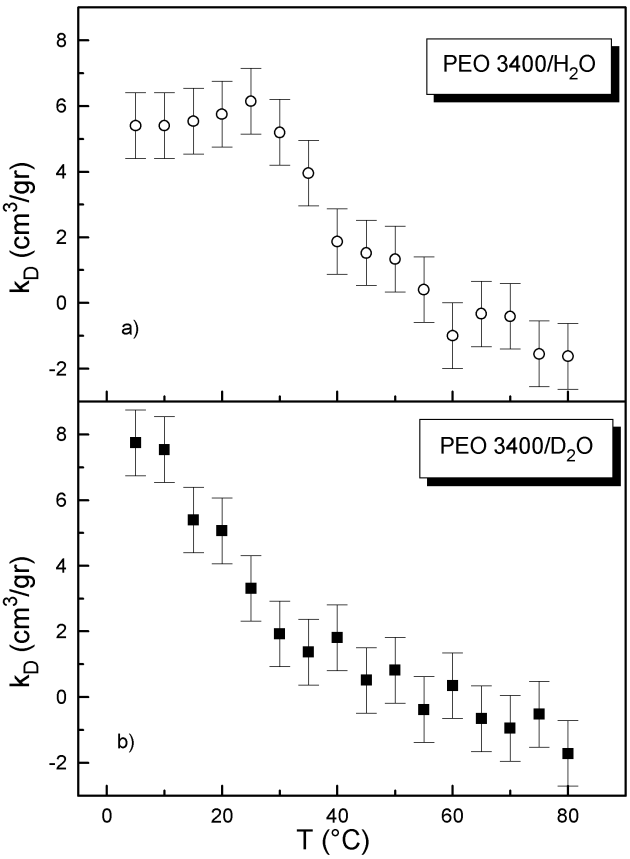

Figure 4. (a) Temperature dependence of k_D for PEO 3400/H_2O solutions. (b) Temperature dependence of k_D for PEO 3400/D_2O solutions.

Sakurada parameters, K and a, in the scaling law relating the intrinsic viscosity $[n]$ to M_w:

$$[\eta] = K M_w^a. \tag{16}$$

The K and a behaviour, as reported in the literature [1], indicates that from 10 to 35 °C water becomes a better solvent, from 35 to 45 °C it approaches its limiting value and, finally, the water solvent power begins to decrease above 45 °C. This behaviour is reflected in the measured k_D temperature dependence, even if friction effects, which are known to be large for PEO in water [7, 33], must be taken into account (equation (8)).

Figure 5 shows, in a log–log plot, the dependence of the PEO diffusion coefficient extrapolated at infinite dilution D_0 on M_w, at $T = 25\,^{\circ}$C. The data, which include results previously obtained [34], fall along a straight line yielding a scaling exponent of $\nu = 0.57$. This value is slightly lower than the one previously obtained without the data for the $M_w = 3400$ sample. This finding can be attributed to the fact that PEO 3400 has not fully reached the asymptotic good solvent behaviour. However it is relevant that in PEO aqueous solutions the scaling law connecting D_0 and M_w holds in the range 3400–4 000 000 Da with a scaling exponent close to the value of 0.588 [35–37] predicted by the theory for a swollen coil in a *good solvent*.

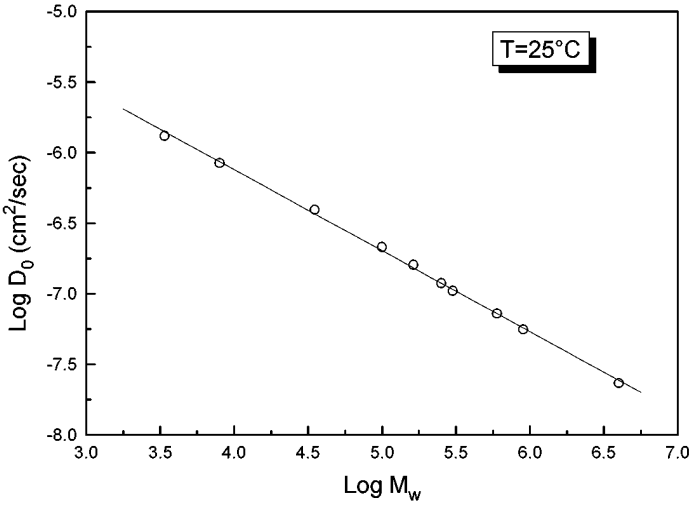

Figure 5. Log–log plot of D_0 as a function of M_w for PEO/H_2O solutions. The straight line represents the best fit according to the scaling law $D_0 = AM_w^{\nu}$ ($\nu = 0.57$).

The interpretation of PCS data is in accordance with the results of Raman measurements. In figure 6, for example, the D-LAM spectra of a PEO 3400/H_2O and of a PEO 3400/D_2O solutions are reported. The continuous and dashed lines represent the best fit according to equation (11). In figure 7 the evolution of the fit parameters $\omega_{D\text{-}LAM}$ and $\gamma_{D\text{-}LAM}$ is reported as a function of n_w/n_p ratio, for the PEO 3400/H_2O and PEO 3400/D_2O solutions, n_w and n_p being the number of water and polymer molecules respectively. As far as the PEO 3400/light water system is concerned, it is evident that, increasing the water content, a remarkable frequency increase (over 10 cm^{-1}) towards values corresponding to those of the crystal phase takes place. On the other hand the diminishing of $\gamma_{D\text{-}LAM}$ clearly indicates the sharpening of the spectral contribution. This evidence is in agreement with the assumption, already mentioned in the introduction, that PEO in water tends to assume, with respect to the melt case, a more ordered conformation, closer to the crystalline one. The picture that emerges is that the addition of water molecules promotes the formation of more rigid hydrated polymer coils. This gives rise to the $\omega_{D\text{-}LAM}$ increase and can be related to the measured initial decrease of the PEO/water compressibility [14] as the water content is raised starting from the pure polymer system. The same hydration process destroys the intermolecular interactions among the polymeric chains and promotes the sharpening of the D-LAM contribution, until, essentially, only one intense band, corresponding to the isolated hydrated polymer coil, is found. In this interpretation the plateau region in figure 7 begins when the number of water molecules per PEO molecule is enough to assure a full hydration of the polymer. The hydration number n_H, as obtained by ultrasonic velocity measurements, agrees with this interpretation of the Raman spectra.

A similar analysis has been carried out for the temperature dependence of the D-LAM contribution. In figure 8 the $\omega_{D\text{-}LAM}$ and $\gamma_{D\text{-}LAM}$ parameters are reported for a PEO + 200 H_2O system as a function of temperature. The chosen concentration corresponds to the plateau zone for $\omega_{D\text{-}LAM}$ and $\gamma_{D\text{-}LAM}$ assuring both a complete hydration of the polymer and a sufficient optical contrast for a good signal-to-noise ratio. As shown, increasing temperature from 10 to 45 °C a small frequency shift towards lower values and a significant broadening of the D-LAM mode is recorded. At higher temperatures, however, one observes an inversion in the behaviours of the $\omega_{D\text{-}LAM}$ and $\gamma_{D\text{-}LAM}$ parameters. Such data indicate, in the 10–45 °C range,

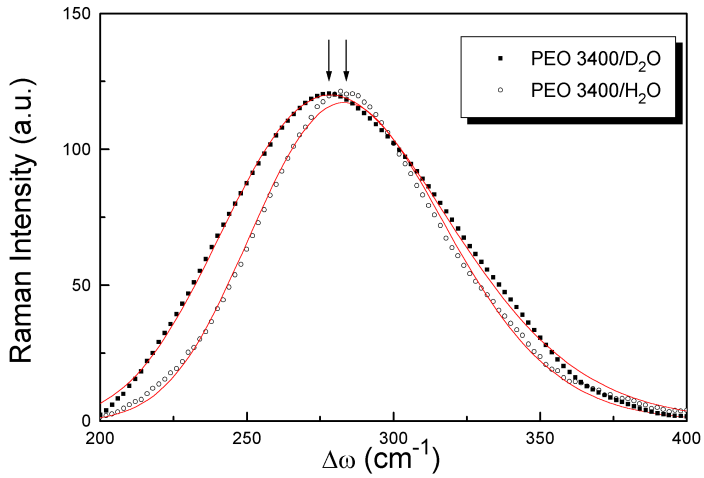

Figure 6. D-LAM contributions for a PEO 3400/H_2O solution (open circles) and for a PEO 3400/D_2O solution (closed squares) at 60 °C. The lines among the experimental points represent the best fit according to equation (11). The arrows indicate the D-LAM centre frequencies.

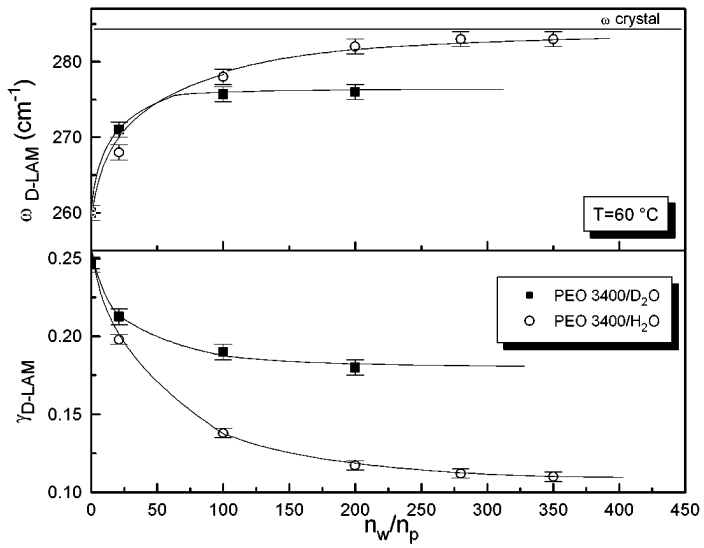

Figure 7. Concentration dependence of the D-LAM centre frequency ($\omega_{D\text{-}LAM}$) and width ($\gamma_{D\text{-}LAM}$) for the PEO 3400/H_2O solutions (open circles) and for the PEO 3400/D_2O solutions (closed squares) at 60 °C. The lines are guides for the eye.

a broadening of the Kuhn length distribution towards higher values. We interpret these results in terms of the effect of the solvent power evolution of H_2O.

It is well known that SANS represents a powerful technique, complementary to the previously reported ones. In order to examine thoroughly the PEO/water system and to introduce the comparison with the PEO/D_2O solutions, SANS measurements in the PEO 3400/heavy water system have been performed at three different temperatures. In figure 9(a) the coherent differential scattering cross sections are reported at $T = 40$ °C as an example. The

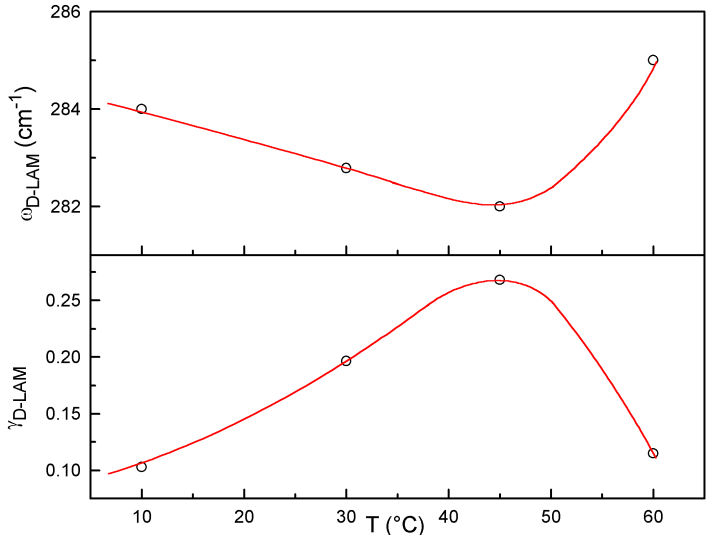

Figure 8. Temperature dependence of the D-LAM centre frequency ($\omega_{D\text{-}LAM}$) and width ($\gamma_{D\text{-}LAM}$) for the solution PEO 3400 + 200 H_2O. The lines are guides for the eye.

spectrum profile is in agreement with the one reported in literature for a solution of PEO 21000 in D_2O [38]. In the low-k region the decrease in the intensity with the increase of polymer concentration reflects the contribution of the interactions between polymer. In the high-k region, where correlations between polymer segments over shorter length scales determine the scattered intensity, the magnitudes of the scattered neutron intensities rank in the opposite order with increasing polymer concentration. This follows from the fact that in the large-k limit, the nature of the correlations within each polymer coil is relatively insensitive to polymer concentration, and each polymer coil acts as an independent scatterer. Consequently, the scattered intensity is simply proportional to the polymer concentration [38]. These occurrences are shown in figure 9(b) which shows the spectra normalized to concentration. As it can be seen, in the low-k region the scattered intensity decreases with increasing concentration and in the high-k limit the normalized spectra superimpose. In figure 9(a) the continuous lines are the fit according to the random coil form factor (equation (13)). In table 2 the obtained values of R_g for all concentrations and temperatures are reported. The apparent values of R_g decrease with increasing concentration indicating repulsive intermolecular interactions. It is important to note that the apparent values of R_g, obtained by fitting the spectra at higher concentration, decrease nonlinearly with increasing PEO concentration. If the conformation of the macromolecules does not change with concentration, the excluded volume effect would lead to a linear decrease in R_g as a function of polymer concentration. The nonlinear variation of R_g observed for PEO may be due to the combined effects of possible changes in the three-dimensional structure and to the interparticle interaction of PEO coils at high concentration [38, 39]. As a consequence, it is expected that SANS spectra are sensitive to the isolated coil and can furnish a value of R_g only in the most dilute solutions. At higher concentrations in the semidilute region, $c > c^*$, polymer coils begin to entangle and the R_g values obtained, more properly, are to be considered static correlation lengths, ξ [39].

To obtain a quantitative estimation of the interparticle interaction the Zimm plot has been used. In figure 10 the quantity $c/I(0)$ is reported as a function of concentration at different temperatures, where $I(0)$ is the intensity extrapolated at zero wave-vector. It is evident that

Table 2. Resulting fit parameters using the Debye form factor for the SANS measurements on PEO 3400/D_2O solutions. A is the amplitude parameter.

	$c = 0.07$ g cm^{-3}		$c = 0.09$ g cm^{-3}		$c = 0.13$ g cm^{-3}		$c = 0.19$ g cm^{-3}		$c = 0.29$ g cm^{-3}	
T (°C)	A	R_g (nm)	A	R_g (nm)	A	R_g (nm)	A	R_g (nm)	A	R_g (nm)
20	0.58	1.25	0.56	1.15	0.53	0.95	0.42	0.74	0.30	0.50
40	0.76	1.42	0.74	1.30	0.71	1.12	0.59	0.90	0.41	0.65
60	1.02	1.58	1.05	1.51	1.05	1.32	0.89	1.07	0.66	0.79

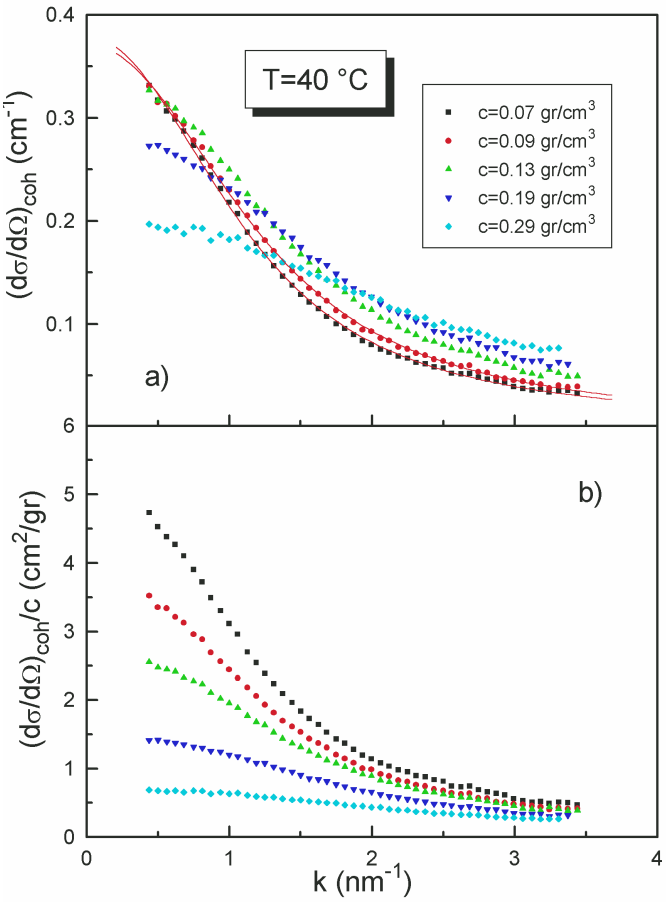

Figure 9. (a) Coherent differential scattering cross section for PEO 3400/D_2O solutions at $T = 40$ °C. (b) Coherent differential scattering cross section normalized to concentration for PEO 3400/D_2O solutions at $T = 40$ °C.

a linear dependence on concentration is not suitable for the analysis. However, using the procedure described in the experimental section, the value of A_2 has been obtained using a linear regression to the three most diluted concentrations for the data extrapolated to $k = 0$ (see figure 10). The obtained values of A_2 as a function of temperature are reported in figure 11. As can be seen A_2 decreases with increasing temperature indicating a lowering of the solvent power of D_2O as the temperature increases. This finding is in contrast with the k_D behaviour

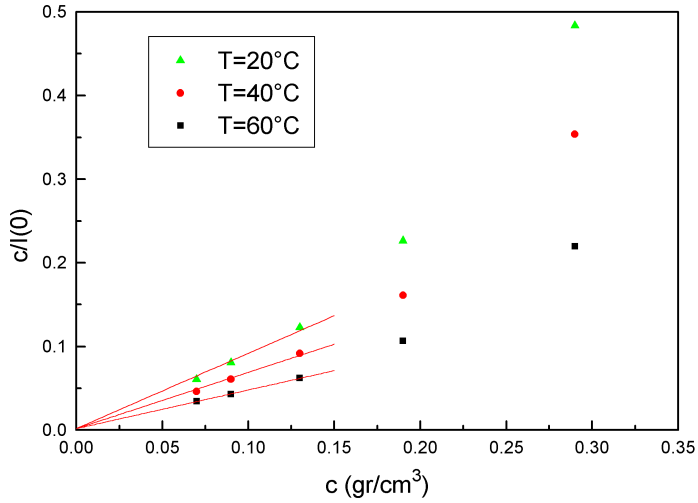

Figure 10. $c/I(0)$ as a function of concentration at different temperatures.

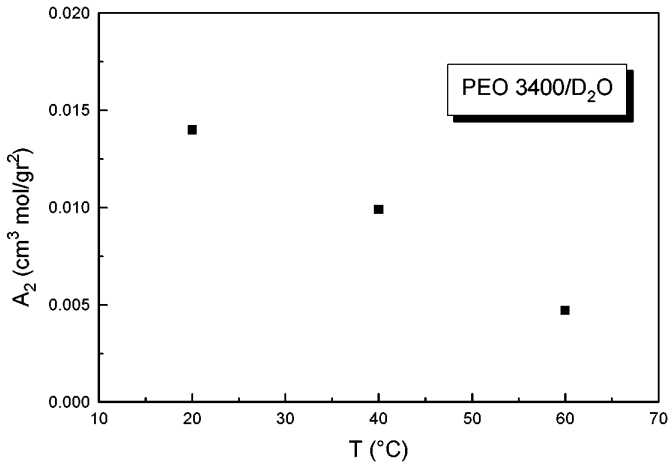

Figure 11. Temperature dependence of A_2 for PEO 3400/D_2O solutions.

obtained for PEO 3400/H_2O solutions; however this result could be attributed to the different isotopic nature of the solvent. It will be shown that this hypothesis is confirmed by PCS measurements on PEO 3400/D_2O solutions. In figure 12 the evaluated radii of gyration are reported as a function of temperature for the most diluted concentration. It can be clearly seen that R_g increases with temperature. This occurrence could be attributed to the fact that, even at the lowest concentration, 0.07 g cm^{-3}, R_g values are to some extent diminished by the repulsive interaction between the chains. Moreover, a comparison between the magnitude of k_D and A_2 reveals that the friction coefficient virial coefficient, k_f, must be unusually large. This finding is in agreement with previous measurements on PEO/H_2O solutions [7].

For a direct comparison with the PEO/light water solutions a series of PCS and Raman measurements on the PEO 3400/D_2O system have been also performed. The effective diffusion coefficient data are reported in figure 13 as a function of concentration at the same temperatures

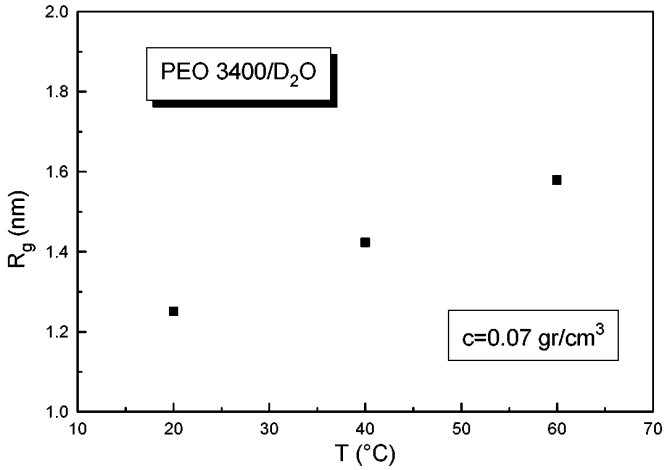

Figure 12. Temperature dependence of the gyration radius for PEO 3400/D_2O solutions.

as in figure 2. Straight lines are the best linear fit according to equation (7). A comparison with the diffusion data on PEO/H_2O solutions reveals that, in heavy water, PEO coils have a lower diffusion coefficient. This occurrence could be ascribed simply to the different rheological properties of the solvent; in fact, at 5 °C D_2O shear viscosity is ∼30% higher than H_2O, this difference slightly decreasing as temperature is raised to a value of ∼15% at 100 °C [40]. This explanation is not fully satisfactory. In figure 3(b) the hydrodynamic radius, as obtained from the ES relation, as a function of temperature is shown. Hydrodynamic radius data reveal a slightly different behaviour, both in the magnitude and in the temperature dependence. At low temperatures, in D_2O, R_H values are slightly higher than in H_2O and remain nearly constant as temperature is raised; in the temperature range of 25–40 °C, polymer dimension decreases and then reaches a constant value, slightly lower than in H_2O at the same temperatures. The temperature dependence of the solvent quality of D_2O turns out to be different from the one in H_2O. It must be stressed that at higher temperatures R_H, both in H_2O and in D_2O, tends to be independent of temperature. This occurrence can be related to the decrease of the hydration number, due to the enhanced thermal motion, and to the lowering of the solvent power incidence.

These findings suggest that the isotopic substitution affects the solvent properties and their dependence on temperature. The increasing of the gyration radius and the decreasing of A_2, as evaluated from the SANS data, in the temperature range 20–60 °C support this hypothesis. Also the evaluation of k_D reveals a different behaviour of the two solvents. In figure 4(b) the k_D values are reported as a function of temperature for the PEO/D_2O system. In agreement with the R_H and A_2 behaviour, k_D decreases with temperature in all the investigated range. In particular, starting from values slightly higher than in H_2O it decreases until, in the range 40–80 °C, no appreciable difference, both in the behaviour and in the numerical values, can be noted. In addition, from the comparison between the R_H and k_D data it seems that their whole behaviours in D_2O are shifted towards lower temperatures with respect to those in H_2O.

The similarity of the temperature dependence of k_D and A_2, evaluated using PCS and SANS respectively, suggests that k_D can be considered a faithful indicator of the PEO intercoil interactions character, in spite of the dependence on k_f, even at that temperatures not directly probed by SANS measurements.

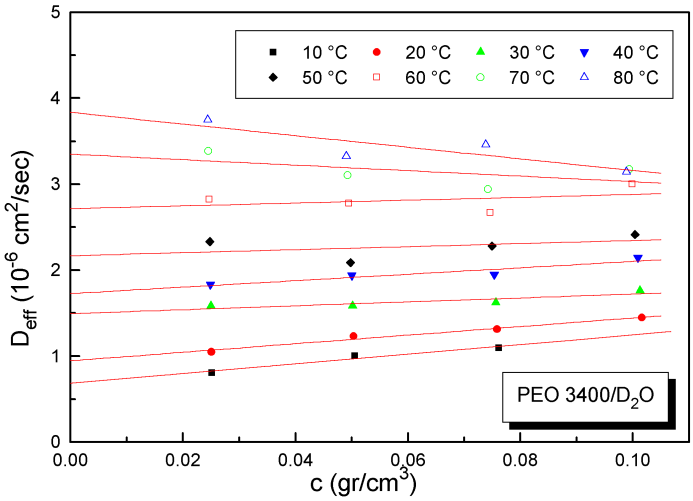

Figure 13. Concentration dependence of the effective diffusion coefficient for PEO 3400/D_2O solutions at various temperatures.

The ratio R_H/R_g furnishes other interesting information about the nature of the solvent–polymer interaction. Treatments based on the assumption of a Gaussian chain predict values of R_H/R_g about 1.5 [41, 42]. In the good solvent limit the obtained value is of 1.6. Instead Benmouna and Akcasu [43], using Ptisyn's pseudo-Gaussian (blob model) found a higher value for highly swollen chain: $R_H/R_g = 1.9$. Previous investigation [7] on PEO/water solution gave a result of $R_H/R_g = 1.7$, intermediate between the two theoretical predictions, which, however, states the swollen conformation of the PEO chain in water solution. In figure 14 the R_H/R_g ratio, as obtained from PCS and SANS measurements, is reported as a function of temperature. The obtained values decrease with temperature from $R_H/R_g = 1.5$ at 20 °C to $R_H/R_g = 1.1$ at 60 °C showing, in agreement with the previous results, a lowering of the solvent power. The comparison with the data of Devanand and Selser [7] indicates that D_2O is a worse solvent with respect to water, even if it must be stressed that the cited results of $R_H/R_g = 1.7$ in the PEO/water system were obtained for higher molecular weight than 3400 Da; indeed a slightly lower value of the R_H/R_g ratio could be due to the fact that PEO 3400 has not yet fully reached asymptotic good solvent behaviour.

The different solvent behaviour of water and heavy water can be shown also by examining the Raman D-LAM contribution. In figure 7 the $\omega_{D\text{-}LAM}$ and $\gamma_{D\text{-}LAM}$ behaviours as functions of concentration for PEO 3400/D_2O solutions are reported and compared to those for the PEO 3400/H_2O solutions at 60 °C. The most striking feature is that in the case of PEO/D_2O solutions, by adding heavy water molecules, the D-LAM centre frequency tends to an asymptotic value smaller than that relative to the PEO/H_2O system. Such a behaviour clearly indicates that the PEO chain conformation in the presence of heavy water is less close to the one of the crystalline phase with respect to the case of the PEO/H_2O system. In addition, if we focus attention on the concentration dependence of the distribution width, a remarkably higher degree of disorder can be demonstrated supporting once more a markedly different behaviour of the PEO/H_2O and PEO/D_2O systems. In fact, the width of the distribution, related to the variety of the different conformers existing in the sample, never approaches the value obtained in the case of the PEO/H_2O system, keeping always a higher value. Moreover,

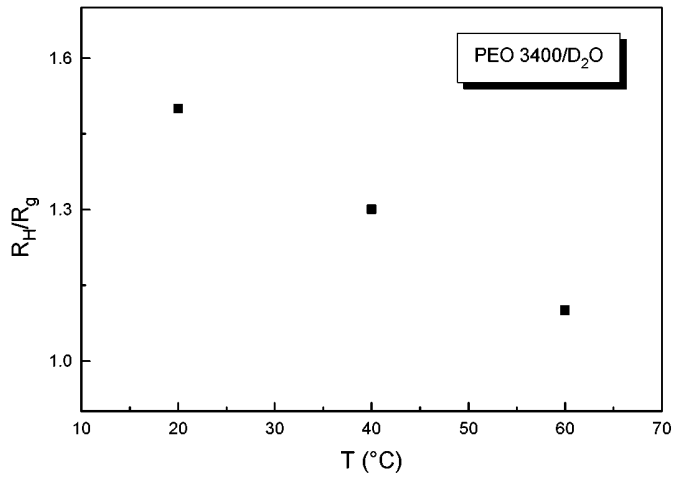

Figure 14. Temperature dependence of R_H/R_g for PEO 3400/D_2O solutions.

$\omega_{D\text{-}LAM}$ begins to saturate at lower n_D/n_p values, where n_D and n_p are the number of heavy water molecules and polymer molecules respectively; this finding indicates that full hydration is reached at lower water content so that the hydration number is less in D_2O than in H_2O. Again the experimental evidence reveals a direct relation between the hydration of the PEO coil and its conformational properties.

5. Concluding remarks

The paper deals with the conformational properties of PEO in the two solvents H_2O and D_2O, investigated by the joint employment of different techniques. It is shown that the solvent quality of PEO/light water–heavy water solutions depends on temperature: first increasing and then decreasing in the PEO/H_2O system; always decreasing with temperature in the PEO/D_2O system. This behaviour has been related to the net result of different occurrences strictly connected with the formation and the rupture of the polymer coil hydration shell and of the H-bond network in the bulk solvent. In particular, it is well known that hydrogen bonding is stronger in D_2O than in H_2O, so that the energy gain for the formation of a bond between PEO and the solvent is lower in D_2O than in H_2O. This occurrence could explain the results reported in the present paper; in fact in the Matsuyama–Tanaka theory, a decrease of the energy gain due to the formation of a physical bond between solute and solvent leads the curve of A_2 as a function of T to lower values and shifts it toward lower temperatures, as experimentally detected by our PCS and Raman analysis.

In conclusion, the present work shows that, besides being lethal for biological systems due to the modification of the H-bond potential well, the isotopic substitution technique, nowadays widely employed in a plenty of structural and dynamical studies, can give rise to different conformational arrangements with markedly different temperature behaviour. These results have a remarkable fall-out on many methodologies available nowadays.

It is well known, for example, that, in designing an experiment to probe molecular structure and dynamics in condensed matter systems, neutron scattering in a wide sense, due to the time–space scale to which it is sensitive and to the simplification brought about by the neutron–nucleus interaction, well meets the necessary requirements. In such a case it is commonly

assumed that the unique distinctive isotope character allows us to select the incoherent or coherent nature of the scattering (that on its own reflects the neutron particle–wave) without any change in the system behavioural properties. What clearly emerges from the present study is that, at least in the PEO–water case, in spite of the great maturity attained in this field, the complexities connected with isotopic substitution, with all its connected drawbacks, limit the effectiveness of the technique that, as a consequence, often requires considerable scrutiny.

References

[1] Bailey F E and Koleske J V 1976 *Poly(Ethylene Oxide)* (New York: Academic)
[2] Molineux P (ed) 1983 *Water-Soluble Synthetic Polymers: Properties and Uses* (Boca Raton, FL: Chemical Rubber Company)
[3] Rabolt J F, Johnson K W and Zitter R N 1974 *J. Chem. Phys.* **61** 504
[4] Miyazawa T 1961 *J. Chem. Phys.* **35** 693
[5] Matsura H. and Fukuhara K 1985 *J. Mol. Struct.* **126** 251
[6] Branca C, Magazù S, Maisano G, Migliardo P and Villari V J 1999 *J. Phys.: Condens. Matter* **10** 10 141
[7] Devanand K and Selser J C 1991 *Macromolecules* **24** 5943
[8] Bieze T W N, Barnes A C, Huige C J, Enderby J E and Leyte J C 1994 *J. Phys. Chem.* **98** 6568
[9] Strazielle C and Benoit H 1975 *Macromolecules* **8** 203
[10] Graessley W W, Krishnamoorti R, Balsara N P, Fetters L J, Lohse D J, Schulz and Sissano J A 1993 *Macromolecules* **26** 1137
[11] Flory P J 1963 *Statiscal Mechanics of Chain Molecules* (New York: Wiley–Interscience)
[12] Flory P J 1941 *J. Chem. Phys.* **9** 660
Flory P J 1942 *J. Chem. Phys.* **10** 51
[13] Huggins M L 1941 *J. Chem. Phys.* **9** 440
Huggins M L 1942 *Ann. N.Y. Acad. Sci.* **43** 1
[14] Kjellander R and Florin E 1981 *J. Chem. Soc., Faraday Trans.* I **77** 2053
[15] Karlström G 1985 *J. Phys. Chem.* **89** 4962
[16] Matsuyama A and Tanaka F 1990 *Phys. Rev. Lett.* **65** 341
[17] Maisano G, Majolino D, Migliardo P, Venuto S, Aliotta F and Magazù S 1993 *Mol. Phys.* **78** 421
[18] Bekiranov S, Bruinsma R and Pincus P 1997 *Phys. Rev.* E **55** 577
[19] Pusey P N 1974 *Photon Correlation and Light Beating Spectroscopy* ed H Z Cummins and E R Pike (New York: Plenum) p 387
[20] Segrè P N, Beherend O P and Pusey P N 1995 *Phys. Rev.* E **52** 5070
[21] Schaefer D W and Han C C 1985 Quasielastic light scattering from dilute and semidilute polymer solution *Dynamic Light Scattering* ed R Pecora (New York: Plenum) p 181
[22] Chu B 1981 *Static and Dynamic Properties of Polymer Solutions (NATO Advanced Study Institute Service Series B 73)* (London: Plenum) p 231
[23] Nishide H, Ohyanagi M, Okada O and Tsuchida E 1986 *Macromolecules* **19** 496
[24] Kim I and Krimm S 1996 *Macromolecules* **29** 7186
[25] Snyder R G and Strauss H L 1987 *J. Chem. Phys.* **87** 3779
[26] Scherer J R and Snyder R G 1980 *J. Chem. Phys.* **72** 5798
[27] Snyder R G, Schlotter N E, Alamo R and Mandelkern L 1986 *Macromolecules* **19** 621
[28] Teixeira J 1992 Introduction to small angle neutron scattering applied to colloidal science *Structure and Dynamics of Strongly Interacting Supramolecular Aggregates in Solution* ed S-H Chen *et al* (Dordrecht: Kluwer)
[29] Debye P 1946 *J. Chem. Phys.* **14** 636
[30] Berne B J and and Pecora R 1976 *Dynamic Light Scattering; With Application to Chemistry, Biology and Physics* (New York: Wiley)
[31] Segrè P N and Pusey P N 1996 *Phys. Rev. Lett.* **77** 771
[32] Klein R and Nägele G 1994 *Nuovo Cimento* **16** 963
[33] Woodley D M, Dam C, Lam H, Le Cave M, Devanand K and Selser J C 1982 *Macromolecules* **25** 5283
[34] Faraone A, Magazù S, Maisano G, Migliardo P, Tettamanti E and Villari V 1999 *J. Chem. Phys.* **109** 1801
[35] Le Guillou J C and Zinn-Justin J 1977 *Phys. Rev. Lett.* **39** 95
[36] McKenzie D S 1976 *Phys. Rep.* C **27** 35
[37] Weill G and des Cloizeaux J 1979 *J. Physique* **40** 99
[38] Thiyagarajan P, Chaiko D J and Hjelm R P Jr 1995 *Macromolecules* **28** 7730
[39] Abbott N L, Blankschtein D and Hatton T A 1992 *Macromolecules* **25** 3932

[40] Jarzynski J and Davis C M 1972 The viscosity of water *Water and Aqueous Solutions: Structure, Thermodynamics, and Transport Processes* ed R A Horne (New York: Wiley–Interscience) p 701 and references therein
[41] Kirkwood J C 1954 *J. Polym. Sci.* **12** 1
[42] Akcasu A G and Gurol H J 1976 *J. Polym Sci., Polym. Phys Edn* **14** 1
[43] Benmouna M and Ackasu A Z 1980 *Macromolecules* **13** 409